Journal of Sandwich Structures and Materials
http://jsm.sagepub.com/

Three-dimensional elasticity solution for sandwich beams/wide plates with orthotropic phases: The negative discriminant case

George A. Kardomateas and Catherine N. Phan

Journal of Sandwich Structures and Materials 2011 13: 641
DOI: 10.1177/1099636211419127

The online version of this article can be found at:
http://jsm.sagepub.com/content/13/6/641

Published by:
SAGE
http://www.sagepublications.com

JOURNAL OF SANDWICH STRUCTURES & MATERIALS

Original Article

Journal of Sandwich Structures and Materials
13(6) 641–661

DOI: 10.1177/1099636211419127
jsm.sagepub.com
SAGE

Three-dimensional elasticity solution for sandwich beams/wide plates with orthotropic phases: The negative discriminant case

George A. Kardomateas and Catherine N. Phan

Abstract

In an earlier paper, Pagano (1969) [Pagano NJ. Exact solutions for composite laminates in cylindrical bending. *J Compos. Mater.* 1969; 3: 398–411] presented the three-dimensional elasticity solution for orthotropic beams (applicable also to sandwich beams) for the cases of: (1) a phase with positive discriminant of the qudratic characteristic equation, which is formed from the orthotropic material constants and further restricted to positive real roots and (2) an isotropic phase, which results in a zero discriminant. The roots in this case are all real, unequal, and positive (positive discriminant) or all real and equal (isotropic case). This purpose of this article is to present the corresponding solution for the cases of (1) negative discrimnant, in which case the two roots are complex conjugates and (2) positive discriminant but real negative roots. The case of negative discriminant is frequently encountered in sandwich construction, where the orthotropic core is stiffer in the transverse than the in-plane directions. Example problems with realistic materials are solved and compared with the classical and the first-order shear sandwich beam theories.

Keywords

beam, elasticity, sandwich, face sheet, core, orthotropic, panel

Introduction

Elasticity solutions are significant because they provide a benchmark for assessing the performance of various beams, plate, or shell theories or the various numerical

School of Aerospace Engineering, Georgia Institute of Technology, Atlanta, GA 30332-0150, USA

Corresponding author:
George A Kardomateas, School of Aerospace Engineering, Georgia Institute of Technology, Atlanta, GA 30332-0150, USA
Email: george.kardomateas@aerospace.gatech.edu

methods such as the finite element method. For monolithic anisotropic bodies, such solutions have been developed primarily by Lekhnitskii [1]. For laminated composite or sandwich structures, a few closed-form solutions exist, namely by Vlasov [2] for isotropic plates, by Pagano [3,4] for beam and plate configurations, respectively (both under restrictive assumptions), and for a sandwich shell configuration by Kardomateas [5]. The purpose of this study is to extend the study for the three-dimensional elastic solution of a laminated beam by Pagano [3].

Specifically, the material constants of each phase (layer in composites or face sheet or core in sandwich) result in a quadratic characteristic equation. In Ref. [3], only the case of positive discriminant of the quadratic equation, which is the case of two unequal real roots, and only when these roots are positive, was treated. The isotropic case, in which there are two equal real roots, was also outlined. In the article, we present the solution for the case of negative discriminant, which results in two complex conjugate roots of the quadratic equation. In addition, we present the solution for a positive discriminant but with real negative roots. Although the case of positive discriminant is probably more frequent with composite layers, the negative discriminant seems to appear frequently in sandwich construction with orthotropic cores, in which the stiffness in the transverse direction is greater than that of the in-plane directions (e.g., realistic honeycomb cores as shown in the example in the results section). Therefore, the solution given in this article completes Pagano's original work [3] for all cases of material constants.

Elasticity formulation

We consider a sandwich beam consisting of orthotropic face sheets of thickness f_1 and f_2 and an orthotropic core of thickness $2c$, such that the various axes of elastic symmetry are parallel to the plate axes x, y, and z (Figure 1). The body is simply

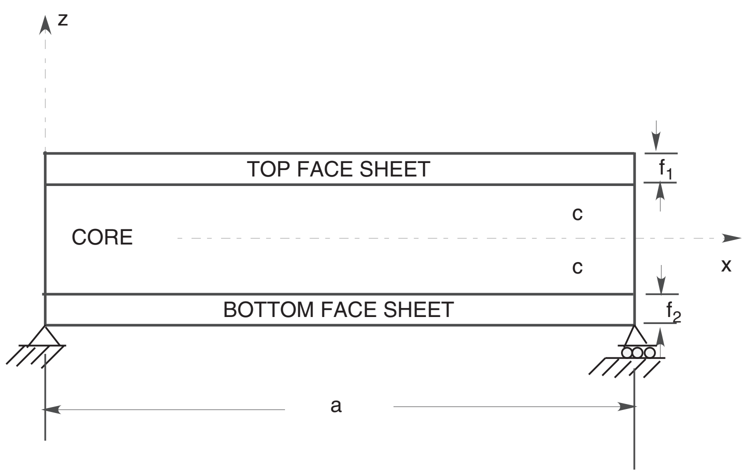

Figure 1. Definition of the geometry and coordinate system for the sandwich beam.

supported. Although the elasticity solution is derived for any loading, results will be presented for a transverse distributed loading $\tilde{q}_0(x)$ applied on the upper surface.

Let us denote each phase by i, where $i = f_1$ for the upper face-sheet, $i = c$ for the core, and $i = f_2$ for the lower one. The displacements along x, y, and z are denoted by u, v, and w, respectively.

The underlying assumption of the problem (one-dimensional) is

$$v = 0; \qquad u, w = \text{fn}(x, z). \tag{1a}$$

Using the strain–displacement relations results in:

$$\epsilon_{xx} = u_{,x}; \qquad \epsilon_{zz} = w_{,z}\ ; \qquad \gamma_{xz} = u_{,z} + w_{,x}, \tag{1b}$$

and

$$\epsilon_{yy} = \gamma_{xy} = \gamma_{yz} = 0. \tag{1c}$$

Then, for each phase, the orthotropic strain–stress relations are:

$$\begin{bmatrix} \sigma_{xx}^{(i)} \\ \sigma_{yy}^{(i)} \\ \sigma_{zz}^{(i)} \\ \tau_{yz}^{(i)} \\ \tau_{xz}^{(i)} \\ \tau_{xy}^{(i)} \end{bmatrix} = \begin{bmatrix} c_{11}^i & c_{12}^i & c_{13}^i & 0 & 0 & 0 \\ c_{12}^i & c_{22}^i & c_{23}^i & 0 & 0 & 0 \\ c_{13}^i & c_{23}^i & c_{33}^i & 0 & 0 & 0 \\ 0 & 0 & 0 & c_{44}^i & 0 & 0 \\ 0 & 0 & 0 & 0 & c_{55}^i & 0 \\ 0 & 0 & 0 & 0 & 0 & c_{66}^i \end{bmatrix} \begin{bmatrix} \epsilon_{xx}^{(i)} \\ 0 \\ \epsilon_{zz}^{(i)} \\ 0 \\ \gamma_{xz}^{(i)} \\ 0 \end{bmatrix}, \quad (i = f_1, c, f_2) \tag{2}$$

where c_{ij}^i are the stiffness constants (we have used the notation $1 \equiv x$, $2 \equiv y$, and $3 \equiv z$).

Accordingly, the non-zero stresses depend only on x and z. Thus, the equilibrium relations are:

$$\sigma_{xx,x} + \tau_{xz,z} = 0, \tag{3a}$$

$$\tau_{xz,x} + \sigma_{zz,z} = 0, \tag{3b}$$

This leads to the following governing field equations in terms of the displacements for each of the phases:

$$c_{11}^i u_{,xx} + c_{55}^i u_{,zz} + (c_{13}^i + c_{55}^i) w_{,xz} = 0, \tag{4a}$$

$$(c_{13}^i + c_{55}^i) u_{,xz} + c_{55}^i w_{,xx} + c_{33}^i w_{,zz} = 0. \tag{4b}$$

In the following, we shall drop the superscript i that refers to the phases (core or face sheets) with the understanding that the derived relations will hold within each phase.

For a simply supported plate, an appropriate solution for the displacements would be in the form:

$$u = U(z)\cos px; \quad w = W(z)\sin px; \quad \text{where} \quad p = \frac{n\pi}{a} \ (n = 1, 2, \ldots). \tag{5a}$$

Note that these displacements, in conjunction with the corresponding forms (1) and (2) stresses, would satisfy the simple support edge conditions.

Assuming next that

$$[U(z), W(z)] = [U_0, W_0]e^{sz}, \tag{5b}$$

where U_0 and W_0 are constants, and substituting (5a, b) into (4) results in the following system of algebraic equations

$$(c_{11}p^2 - c_{55}s^2)U_0 - (c_{13} + c_{55})psW_0 = 0, \tag{6a}$$

$$(c_{13} + c_{55})psU_0 + (c_{55}p^2 - c_{33}s^2)W_0 = 0. \tag{6b}$$

Non-trivial solutions of this system exist only if the determinant of the coefficients vanishes, which leads to the equation:

$$A_0s^4 + A_1s^2 + A_2 = 0, \tag{7}$$

where

$$A_0 = c_{33}c_{55}, \quad A_2 = p^4c_{11}c_{55} \tag{8a}$$

$$A_1 = p^2\left[(c_{13} + c_{55})^2 - c_{11}c_{33} - c_{55}^2\right], \tag{8b}$$

With the substitution

$$\lambda = s^2, \tag{9a}$$

Equation (7), which defines the parameter s, can be written in the form of a quadratic equation as:

$$A_0\lambda^2 + A_1\lambda + A_2 = 0. \tag{9b}$$

This is what we would call the characteristic equation for the elasticity solution. The discriminant of this equation is:

$$\Delta = A_1^2 - 4A_0A_2. \tag{10}$$

If $\Delta > 0$, then all roots are real and unequal. If, furthermore, these two real roots are positive, the case was treated by Pagano [3]. We consider next the case of negative discriminant, which has not yet been treated. The case of a positive discriminant with negative real roots will be treated subsequently.

Solution for negative discriminant

If $\Delta < 0$, then the quadratic Equation (10) has two complex conjugate roots:

$$\lambda_1 = \mu_R + i\mu_I; \quad \lambda_2 = \mu_R - i\mu_I; \quad \text{where} \quad \mu_R = -\frac{A_1}{2A_0}; \quad \mu_I = \frac{\sqrt{|\,\Delta\,|}}{2A_0}. \tag{11a}$$

In terms of the modulus r and amplitude θ of these complex numbers,

$$r = \sqrt{\mu_R^2 + \mu_I^2}; \quad \theta = \arctan\left(\frac{\mu_I}{\mu_R}\right), \tag{11b}$$

these roots can be set in the form:

$$\lambda_1 = r(\cos\theta + i\sin\theta); \quad \lambda_2 = r(\cos\theta - i\sin\theta). \tag{11c}$$

From (9), we seek now the square roots of the λ_i's. Thus, in terms of:

$$\gamma_1 = \sqrt{r}\cos\frac{\theta}{2}; \quad \gamma_2 = \sqrt{r}\sin\frac{\theta}{2}, \tag{11d}$$

the corresponding roots of the fourth-order Equation (7), s_i, are:

$$s_{1,2} = \pm(\gamma_1 + i\gamma_2); \quad s_{3,4} = \pm(\gamma_1 - i\gamma_2). \tag{11e}$$

Corresponding to these four roots, the displacement functions take the form:

$$\begin{aligned} U_\eta(z) = {} & a_{1\eta}e^{\gamma_1 z}\cos\gamma_2 z + a_{2\eta}e^{\gamma_1 z}\sin\gamma_2 z \\ & + a_{3\eta}e^{-\gamma_1 z}\cos\gamma_2 z + a_{4\eta}e^{-\gamma_1 z}\sin\gamma_2 z; \quad \eta = u, w, \end{aligned} \tag{12}$$

where $\eta = u, w$ corresponds to the U and W displacements, respectively, and $a_{1\eta}$ are constants.

Of the eight constants appearing in (12) only four are independent. The four relations that exist among these constants are found by substituting the displacements along with (5) into the equilibrium equations (4). For convenience, let us set:

$$r_1 = \frac{\gamma_1\left[c_{11}p^2 - c_{55}(\gamma_1^2 + \gamma_2^2)\right]}{p(c_{13} + c_{55})(\gamma_1^2 + \gamma_2^2)}; \quad r_2 = \frac{\gamma_2\left[c_{11}p^2 + c_{55}(\gamma_1^2 + \gamma_2^2)\right]}{p(c_{13} + c_{55})(\gamma_1^2 + \gamma_2^2)}, \tag{13a}$$

In this way, we obtain the following relations for the coefficients in the displacement expression for $W(z)$, equation (12), in terms of the coefficients in the expression for $U(z)$:

$$a_{1w} = r_1 a_{1u} - r_2 a_{2u}, \qquad a_{2w} = r_2 a_{1u} + r_1 a_{2u}, \tag{13b}$$

$$a_{3w} = -r_1 a_{3u} - r_2 a_{4u}, \qquad a_{4w} = r_2 a_{3u} - r_1 a_{4u}. \tag{13c}$$

Hence, if we consider the constants a_{1u}, a_{2u}, a_{3u}, and a_{4u} as independent, which we rename for convenience as g_1, g_2, g_3, and g_4, respectively, the displacement $u(x, z)$ is in the form

$$u = (d_{u1} g_1 + d_{u2} g_2 + d_{u3} g_3 + d_{u4} g_4) \cos px, \tag{14a}$$

with the z-dependent coefficients defined as:

$$d_{u1} = e^{\gamma_1 z} \cos \gamma_2 z; \qquad d_{u2} = e^{\gamma_1 z} \sin \gamma_2 z, \tag{14b}$$

$$d_{u3} = e^{-\gamma_1 z} \cos \gamma_2 z; \qquad d_{u4} = e^{-\gamma_1 z} \sin \gamma_2 z. \tag{14c}$$

The displacement $w(x, z)$ is in the form:

$$w = (d_{w1} g_1 + d_{w2} g_2 + d_{w3} g_3 + d_{w4} g_4) \sin px, \tag{15a}$$

where the z-dependent coefficients are defined:

$$d_{w1} = (r_1 \cos \gamma_2 z + r_2 \sin \gamma_2 z) e^{\gamma_1 z}; \quad d_{w2} = (r_1 \sin \gamma_2 z - r_2 \cos \gamma_2 z) e^{\gamma_1 z}, \tag{15b}$$

$$d_{w3} = (r_2 \sin \gamma_2 z - r_1 \cos \gamma_2 z) e^{-\gamma_1 z}; \quad d_{w4} = (r_2 \cos \gamma_2 z - r_1 \sin \gamma_2 z) e^{-\gamma_1 z}. \tag{15c}$$

The corresponding stresses are derived by substituting the above displacement expressions into (5), (1), and (2). We present the explicit expressions for the stresses as follows.

The transverse normal stress $\sigma_{zz}(x, z)$ is in the form

$$\sigma_{zz} = (b_{zz1} g_1 + b_{zz2} g_2 + b_{zz3} g_3 + b_{zz4} g_4) \sin px, \tag{16a}$$

with the z-dependent coefficients defined as:

$$b_{zz1} = [c_{33}(r_1\gamma_1 + r_2\gamma_2) - c_{13}p] e^{\gamma_1 z} \cos \gamma_2 z + c_{33}(r_2\gamma_1 - r_1\gamma_2) e^{\gamma_1 z} \sin \gamma_2 z, \tag{16b}$$

$$b_{zz2} = c_{33}(r_1\gamma_2 - r_2\gamma_1) e^{\gamma_1 z} \cos \gamma_2 z + [c_{33}(r_1\gamma_1 + r_2\gamma_2) - c_{13}p] e^{\gamma_1 z} \sin \gamma_2 z, \tag{16c}$$

$$b_{zz3} = [c_{33}(r_1\gamma_1 + r_2\gamma_2) - c_{13}p] e^{-\gamma_1 z} \cos \gamma_2 z - c_{33}(r_2\gamma_1 - r_1\gamma_2) e^{-\gamma_1 z} \sin \gamma_2 z, \tag{16d}$$

and

$$b_{zz4} = c_{33}(r_2\gamma_1 - r_1\gamma_2)e^{-\gamma_1 z}\cos\gamma_2 z + [c_{33}(r_1\gamma_1 + r_2\gamma_2) - c_{13}p]e^{-\gamma_1 z}\sin\gamma_2 z. \tag{16e}$$

The shear stress $\tau_{xz}(x, z)$ is in the form:

$$\tau_{xz} = (b_{xz1}g_1 + b_{xz2}g_2 + b_{xz3}g_3 + b_{xz4}g_4)\cos px, \tag{17a}$$

with the z-dependent coefficients defined as:

$$b_{xz1} = c_{55}e^{\gamma_1 z}[(\gamma_1 + pr_1)\cos\gamma_2 z + (pr_2 - \gamma_2)\sin\gamma_2 z], \tag{17b}$$

$$b_{xz2} = c_{55}e^{\gamma_1 z}[(\gamma_2 - pr_2)\cos\gamma_2 z + (pr_1 + \gamma_1)\sin\gamma_2 z], \tag{17c}$$

$$b_{xz3} = c_{55}e^{-\gamma_1 z}[-(pr_1 + \gamma_1)\cos\gamma_2 z + (pr_2 - \gamma_2)\sin\gamma_2 z], \tag{17d}$$

and

$$b_{xz4} = c_{55}e^{-\gamma_1 z}[(\gamma_2 - pr_2)\cos\gamma_2 z - (pr_1 + \gamma_1)\sin\gamma_2 z]. \tag{17e}$$

Finally, the axial stress σ_{xx} is in the form:

$$\sigma_{xx} = (b_{xx1}g_1 + b_{xx2}g_2 + b_{xx3}g_3 + b_{xx4}g_4)\sin px, \tag{18}$$

where the z-dependent coefficients b_{xxj} are found from the b_{zzj} expressions (16(b)–(e) by replacing c_{33} with c_{13} and c_{13} with c_{11}.

From this analysis, we can see that within each phase (i), where $i = f_1, c, f_2$, there are four constants: $g_j^{(i)}, j = 1,\ldots 4$. Therefore, for the three phases, this gives a total of 12 constants to be determined.

There are two traction conditions at each of the two core/face-sheet interfaces, giving a total of four conditions. In a similar fashion, there are two displacement continuity conditions at each of the two core/face-sheet interfaces, giving another four conditions. Finally, there are two traction boundary conditions on each of the two plate bounding surfaces, giving another four conditions, for a total of 12 equations.

Positive discriminant solution

If the discriminant Δ is positive then the two roots are real and unequal and are as follows:

$$\lambda_1 = \frac{-A_1 + \sqrt{\Delta}}{2A_0}\ ; \qquad \lambda_2 = \frac{-A_1 - \sqrt{\Delta}}{2A_0}, \tag{19a}$$

If we set

$$m_j = \sqrt{|\lambda_j|}\ , \tag{19b}$$

then, if $\lambda_j < 0$, the corresponding two roots of (7) are $s_j = \pm i m_j$, $j = 1, 2$ and from (5b) for each pair of roots s_j, we can write:

$$U(z) = \sum_{j=1}^{2} a_{1j} \cos m_j z + a_{2j} \sin m_j z, \tag{20a}$$

$$W(z) = \sum_{j=1}^{2} b_{1j} \cos m_j z + b_{2j} \sin m_j z, \tag{20b}$$

Of the eight constants that enter into (20), only four are independent. The four relations between these constants are found by substituting (20) directly into (5a) and then into the equilibrium equations (4). This leads to the following two equations for b_{1j} and b_{2j}, $j = 1, 2$:

$$b_{1j} = -\alpha_j a_{2j}; \quad b_{2j} = \alpha_j a_{1j}, \tag{20c}$$

where we have set:

$$\alpha_j = \frac{(c_{55} + c_{13}) p m_j}{c_{33} m_j^2 + c_{55} p^2}. \tag{20d}$$

If on the other hand, $\lambda_j > 0$, then the corresponding two roots of (7) are $s_j = \pm m_j$, $j = 1, 2$ and by following an analogous procedure, we can write:

$$U(z) = \sum_{j=1}^{2} a_{1j} \cosh m_j z + a_{2j} \sinh m_j z, \tag{21a}$$

$$W(z) = \sum_{j=1}^{2} b_{1j} \cosh m_j z + b_{2j} \sinh m_j z, \tag{21b}$$

and the constants in $W(z)$ are expressed in terms of the constants in $U(z)$ as:

$$b_{1j} = -\beta_j a_{2j}; \quad b_{2j} = \beta_j a_{1j}, \tag{21c}$$

where we have set:

$$\beta_j = \frac{(c_{55} + c_{13}) p m_j}{c_{33} m_j^2 - c_{55} p^2}. \tag{21d}$$

Hence, the independent parameters are the four constants a_{11}, a_{12}, a_{21}, and a_{22}, which we rename for convenience as g_1, g_2, g_3, and g_4, respectively. Then, the displacements are as follows:

$$U(z) = (d_{u1}g_1 + d_{u2}g_2 + d_{u3}g_3 + d_{u4}g_4)\cos px, \tag{22a}$$

with the z-dependent coefficients defined for $j = 1, 2$,

$$d_{uj} = \begin{cases} \cos m_j z, & \text{if } \lambda_j < 0 \\ \cosh m_j z, & \text{if } \lambda_j > 0 \end{cases} \tag{22b}$$

$$d_{u(j+2)} = \begin{cases} \sin m_j z, & \text{if } \lambda_j < 0 \\ \sinh m_j z, & \text{if } \lambda_j > 0 \end{cases} \tag{22c}$$

and

$$W(z) = (d_{w1}g_1 + d_{w2}g_2 + d_{w3}g_3 + d_{w4}g_4)\sin px, \tag{23a}$$

where the z-dependent coefficients are again defined for $j = 1, 2$,

$$d_{wj} = \begin{cases} \alpha_j \sin m_j z, & \text{if } \lambda_j < 0 \\ \beta_j \sinh m_j z, & \text{if } \lambda_j > 0 \end{cases} \tag{23b}$$

$$d_{w(j+2)} = \begin{cases} -\alpha_j \cos m_j z, & \text{if } \lambda_j < 0 \\ \beta_j \cosh m_j z, & \text{if } \lambda_j > 0 \end{cases} \tag{23c}$$

The corresponding stresses are derived by substituting the above displacement expressions into (1) and (2). We present the explicit expressions for the σ_{zz}, and τ_{xz}. The σ_{zz} can be written in the form:

$$\sigma_{zz} = (b_{zz1}g_1 + b_{zz2}g_2 + b_{zz3}g_3 + b_{zz4}g_4)\sin px, \tag{24a}$$

with the z-dependent coefficients defined for $j = 1,2$, as:

$$b_{zzj} = \begin{cases} \left(-c_{13}p + c_{33}\alpha_j m_j\right)\cos m_j z, & \text{if } \lambda_j < 0 \\ \left(-c_{13}p + c_{33}\beta_j m_j\right)\cosh m_j z, & \text{if } \lambda_j > 0 \end{cases} \tag{24b}$$

$$b_{zz(j+2)} = \begin{cases} \left(-c_{13}p + c_{33}\alpha_j m_j\right)\sin m_j z, & \text{if } \lambda_j < 0 \\ \left(-c_{13}p + c_{33}\beta_j m_j\right)\sinh m_j z, & \text{if } \lambda_j > 0 \end{cases} \tag{24c}$$

Next,

$$\tau_{xz} = (b_{xz1}g_1 + b_{xz2}g_2 + b_{xz3}g_3 + b_{xz4}g_4)\cos px, \tag{25a}$$

with the z-dependent coefficients defined for $j = 1,2$, as:

$$b_{xzj} = \begin{cases} c_{55}(p\alpha_j - m_j)\sin m_j z, & \text{if } \lambda_j < 0 \\ c_{55}(p\beta_j + m_j)\sinh m_j z, & \text{if } \lambda_j > 0 \end{cases} \tag{25b}$$

$$b_{xz(j+2)} = \begin{cases} c_{55}(m_j - p\alpha_j)\cos m_j z, & \text{if } \lambda_j < 0 \\ c_{55}(p\beta_j + m_j)\cosh m_j z, & \text{if } \lambda_j > 0 \end{cases} \tag{25c}$$

Finally, the axial stress σ_{xx} is in the form (18), where the z-dependent coefficients b_{xxj} are found from the b_{zzj} expressions (24) by replacing c_{33} with c_{13} and c_{13} with c_{11}.

For completeness, we give the complete solution for isotropic phases in Appendix 1. This was outlined in Ref. [3].

Results and discussion

We shall consider sandwich configurations consisting of faces made out of either graphite/epoxy or E-glass/polyester unidirectional composite and core made out of either hexagonal glass/phenolic honeycomb or balsa wood. The moduli and Poisson's ratios for these materials are given in Table 1.

Table 1. Material properties.

	Graphite epoxy FACE	E-glass polyester FACE	Balsa wood CORE	Glass-phenolic honeycomb CORE
E_1	181.0	40.0	0.671	0.032
E_2	10.3	10.0	0.158	0.032
E_3	10.3	10.0	7.72	0.300
G_{23}	5.96	3.5	0.312	0.048
G_{31}	7.17	4.5	0.312	0.048
G_{12}	7.17	4.5	0.200	0.013
ν_{32}	0.40	0.40	0.49	0.25
ν_{31}	0.016	0.26	0.23	0.25
ν_{12}	0.277	0.065	0.66	0.25

Note: Moduli data are in GPa.

The two face sheets are assumed identical with thickness $f_1 = f_2 = f = 2$ mm. The core thickness is $2c = 16$ mm. The total thickness of the plate is defined as $h_{\text{tot}} = 2f + 2c$ and the length of the beam is $a = 20h_{\text{tot}}$. A unit width is assumed.

We further assume that a transverse distributed loading $\widetilde{q}_0(x)$ per unit width is applied at the top face sheet. The form of the distributed load is of the form:

$$\widetilde{q}_0(x) = q_0 \sin\frac{\pi x}{a}, \tag{26a}$$

therefore in the definition of p in (5d), we have $n = 1$. Note that a general loading can be expanded in a series of terms of the type $q_n \sin\frac{n\pi x}{a}$ anyway.

In the following results, the displacements are normalized with

$$w_{\text{norm}} = \frac{3q_0 a^4}{2\pi^4 E_1^f f^3}. \tag{26b}$$

and the stresses with q_0.

For each phase, the stiffness constants c_{ij}, that enter into the solution are found from:

$$c_{11} = E_1\frac{(1 - \nu_{23}\nu_{32})}{C_0}; \quad c_{13} = E_3\frac{(\nu_{13} + \nu_{12}\nu_{23})}{C_0}, \tag{26c}$$

$$c_{33} = E_3\frac{(1 - \nu_{12}\nu_{21})}{C_0}, \quad c_{55} = G_{31}, \tag{27a}$$

where

$$C_0 = 1 - (\nu_{12}\nu_{21} + \nu_{23}\nu_{32} + \nu_{13}\nu_{31}) - (\nu_{12}\nu_{23}\nu_{31} + \nu_{21}\nu_{13}\nu_{32}). \tag{27b}$$

Substituting these into Equation (10) gives the discriminant for each phase and the corresponding λ's depending on whether the discriminant is positive or negative. The elasticity solution for the displacements, stresses, and strains follows accordingly as outlined above in terms of the constants $g_j^{(f2)}$, $g_j^{(c)}$, and $g_j^{(f1)}$, $j = 1, 4$. These 12 constants are determined as follows:

There are two traction conditions at the lower face-sheet/core interface, $z = -c$:

a. The $\sigma_{zz}^{(c)} = \sigma_{zz}^{(f2)}\,|_{z=-c}$, which gives:

$$\sum_{j=1}^{4} b_{zzj}^{(c)}\,|_{z=-c}\, g_j^{(c)} = \sum_{j=1}^{4} b_{zzj}^{(f2)}\,|_{z=-c}\, g_j^{(f2)}, \tag{28a}$$

and

b. the $\tau_{xz}^{(c)} = \tau_{xz}^{(f2)}\,|_{z=-c}$, which gives:

$$\sum_{j=1}^{4} b_{xzj}^{(c)}\,|_{z=-c}\, g_j^{(c)} = \sum_{j=1}^{4} b_{xzj}^{(f2)}\,|_{z=-c}\, g_j^{(f2)}. \tag{28b}$$

There are also two displacement continuity conditions at the lower core/face-sheet interfaces:

(a) The $U^{(c)} = U^{(f2)}$ at $z = -c$, which results in:

$$\sum_{j=1}^{4} d_{uj}^{(c)} \,|_{z=-c}\, g_j^{(c)} = \sum_{j=1}^{4} d_{uj}^{(f2)} \,|_{z=-c}\, g_j^{(f2)}, \tag{28c}$$

and finally
(c) the $W^{(c)} = W^{(f2)}$ at $z = -c$, which gives:

$$\sum_{j=1}^{4} d_{wj}^{(c)} \,|_{z=-c}\, g_j^{(c)} = \sum_{j=1}^{4} d_{wj}^{(f2)} \,|_{z=-c}\, g_j^{(f2)}. \tag{28d}$$

Next, there are two traction conditions at the upper face-sheet/core interface, $z = +c$:

(a) $\sigma_{zz}^{(f1)} = \sigma_{zz}^{(c)} \,|_{z=+c}$, which gives:

$$\sum_{j=1}^{4} b_{zzj}^{(c)} \,|_{z=+c}\, g_j^{(c)} = \sum_{j=1}^{4} b_{zzj}^{(f1)} \,|_{z=+c}\, g_j^{(f1)}, \tag{29a}$$

and
(c) $\tau_{xz}^{(f1)} = \tau_{xz}^{(c)} \,|_{z=+c}$, which gives:

$$\sum_{j=1}^{4} b_{xzj}^{(c)} \,|_{z=+c}\, g_j^{(c)} = \sum_{j=1}^{4} b_{xzj}^{(f1)} \,|_{z=+c}\, g_j^{(f1)}. \tag{29b}$$

The corresponding displacement continuity conditions at the upper face-sheet/core interface, $z = +c$ are:

(a) $U^{(f1)} = U^{(c)}$ at $z = +c$, which gives:

$$\sum_{j=1}^{4} d_{uj}^{(c)} \,|_{z=+c}\, g_j^{(c)} = \sum_{j=1}^{4} d_{uj}^{(f1)} \,|_{z=+c}\, g_j^{(f1)}, \tag{29c}$$

and
(c) $W^{(f1)} = W^{(c)}$ at $z = +c$, which gives:

$$\sum_{j=1}^{4} d_{wj}^{(c)} \,|_{z=+c}\, g_j^{(c)} = \sum_{j=1}^{4} d_{wj}^{(f1)} \,|_{z=+c}\, g_j^{(f1)}. \tag{29d}$$

Finally, two traction conditions exist on each of the two bounding surfaces. The traction free conditions at the lower bounding surface, $z = -(c + f_2)$, can be written as follows:

(a) $\sigma_{zz} \mid_{z=-(c+f2)} = 0$, which gives:

$$\sum_{j=1}^{4} b_{zzj}^{(f2)} \mid_{z=-(c+f_2)} g_j^{(f2)} = 0, \tag{30a}$$

and

(c) $\tau_{xz} \mid_{z=-(c+f2)}$, which gives:

$$\sum_{j=1}^{4} b_{xzj}^{(f2)} \mid_{z=-(c+f_2)} g_j^{(f2)} = 0. \tag{30b}$$

And for the upper bounding surface, where the transverse load q_0 is applied:

(a) $\sigma_{zz} \mid_{z=(c+f1)} = q_0$, which gives:

$$\sum_{j=1}^{4} b_{zzj}^{(f1)} \mid_{z=(c+f1)} g_j^{(f1)} = q_0, \tag{30c}$$

and

(c) $\tau_{xz} \mid_{z=(c+f1)} = 0$, which gives:

$$\sum_{j=1}^{4} b_{xzj}^{(f1)} \mid_{z=(c+f1)} g_j^{(f1)} = 0. \tag{30d}$$

Therefore, we have a system of 12 linear algebraic equations in the 12 unknowns, $g_j^{(f2)}$, $g_j^{(c)}$, and $g_j^{(f1)}$, $j = 1, 4$.

Plotted in Figure 2 is the normalized displacement at the top face sheet as a function of x, for the case of graphite/epoxy faces and glass phenolic honeycomb core. In this figure, we also show the predictions of the simple classical beam theory, which does not include transverse shear, as well as the first-order shear theory; for the latter, there are two versions: one that is based only on the core shear stiffness and one that includes the face sheet stiffnesses. Both are outlined in Appendix 2. From Figure 2, we can see that both the classical and first-order Shear (both versions) seem to be inadequate. The classical theory is too non-conservative and the first-order Shear theory with face sheets included can hardly make a difference. On the other hand, the first-order shear theory, where shear is assumed to be carried exclusively by the core is too conservative. In Figure 2, we can also readily observe the large effect of transverse shear, which is an important feature of sandwich structures. Further and most definite confirmation of these results could be provided by comparison with experimental data, and this is indeed a part of our future research plans.

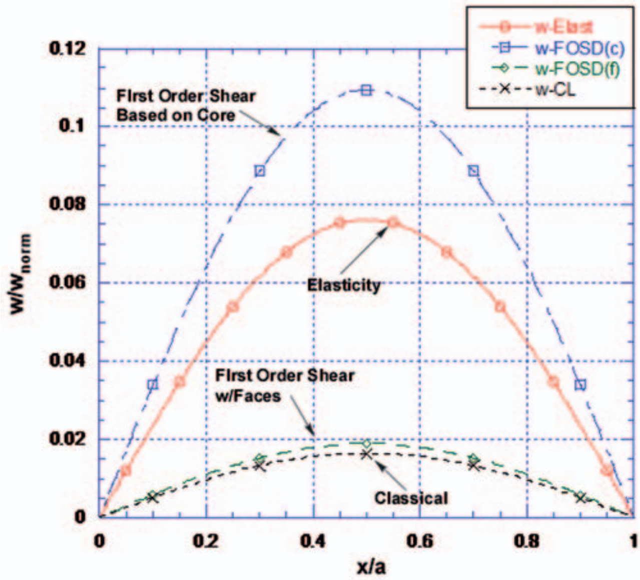

Figure 2. Transverse displacement, *w*, at the top, $z = c + f$, for the case of graphite/epoxy faces and glass phenolic honeycomb core.

The distribution of the axial stress in the core, σ_{xx}, as a function of z at the midspan location, $x = a/2$ (where the bending moment is maximum), is plotted in Figure 3(a), again for the case of graphite/epoxy faces and glass phenolic honeycomb core. The classical and first-order shear theories give practically identical predictions but they are in appreciable error in comparison to the elasticity, the error increasing toward the lower end of the core ($z = -c$). All curves are linear. Notice also that for the elasticity, there is not a symmetry with regard to the midline ($z = 0$) unlike the classical and first-order shear theories.

The effect of different face/core combinations on the axial stress in the core, σ_{xx}, is shown in Figure 3(b), where three face/core combinations (same geometry) are examined. The range of the axial stress is greatly affected by the core; for the same faces, higher axial stress range occurs with the stiffer core. Indeed, when the faces are the same (glass–polyester), the stiffer balsa core case shows a higher range of axial stress in the core than the weaker phenolic core case.

The corresponding three face/core combinations axial strain in the core, ϵ_{xx}, is shown in Figure 3(c). It is interesting to notice that the axial strain is mostly influenced by the faces; for the same core, the stiffer faces result in less axial strain in the core. Indeed, we can observe from Fig. 3(b), that when the core is the same (Phenolic), the less stiff glass/polyester face case shows a higher range of axial stress in the core than the stiffer graphite/epoxy case.

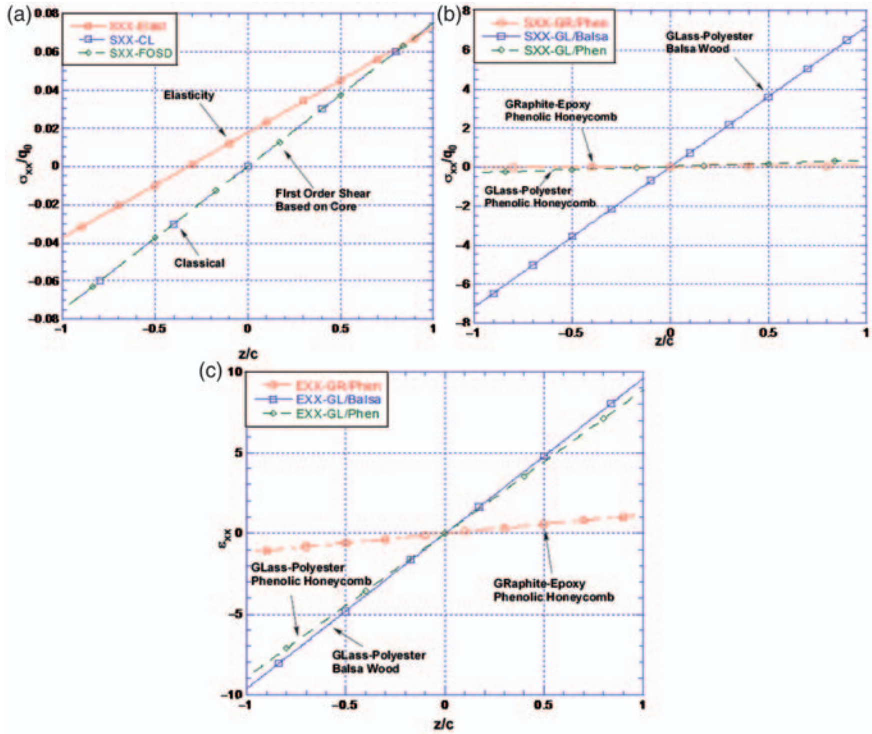

Figure 3. Through-thickness distribution in the core of; (a) the axial stress, σ_{xx}, at $x = a/2$ for; (a) the case of graphite/epoxy faces and glass phenolic honeycomb core, (b) axial stress, ϵ_{xx}, at $x = a/2$ for three face/core material combination, and (c) the axial strain, ϵ_{xx}, at $x = a/2$, for three face/core material combinations.

The through-thickness distribution of the transverse normal stress in the core, σ_{zz}, at the midspan location, $x = a/2$, is shown in Figure 4(a) for three face/core combinations (same geometry). Only the profiles from the elasticity solution are shown, since the first-order shear theory and the classical theory consider the core incompressible, i.e., zero σ_{zz}. It is worth observing that the transverse normal stress is practically the same in all three cases and all are nearly linear.

However, the theories differ when the transverse normal strain is examined in Figure 4(b). We can see that the normal strain profile is strongly influenced by the core; for the same faces, lower normal strains occur with the stiffer core. We can observe from Figure 4(b) that when the faces are the same (glass–polyester), the weaker phenolic core case shows higher normal strains in the core than the stronger balsa core case. Also, we can observe that when the core is the same, there is little influence of the face sheet with the graphite/epoxy and glass/polyester faces, both with the same phenolic core being very similar.

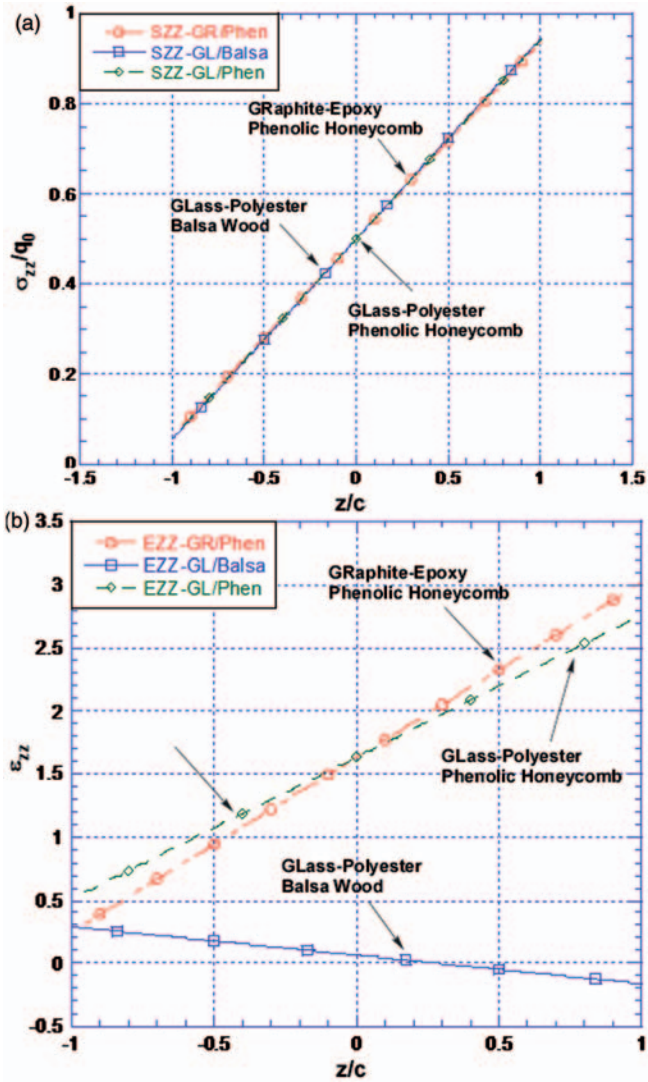

Figure 4. Through-thickness distribution in the core of the transverse normal stress (a) σ_{zz}, at $x = a/2$, for three face/core material combinations. (b) transverse normal strain, ϵ_{zz}, at $x = a/2$, for three face/core material combinations.

Figure 5 shows the through-thickness distribution of the transverse shear stress in the core, τ_{xz}, at $x = a/10$, i.e., near the ends, where shearing is expected to be significant, for the three face/core combinations (same geometry). For the very soft core cases, the shearing stress is nearly constant. However, for the case of the stiffer Balsa core, the shear stress shows a noticeable distribution through the thickness.

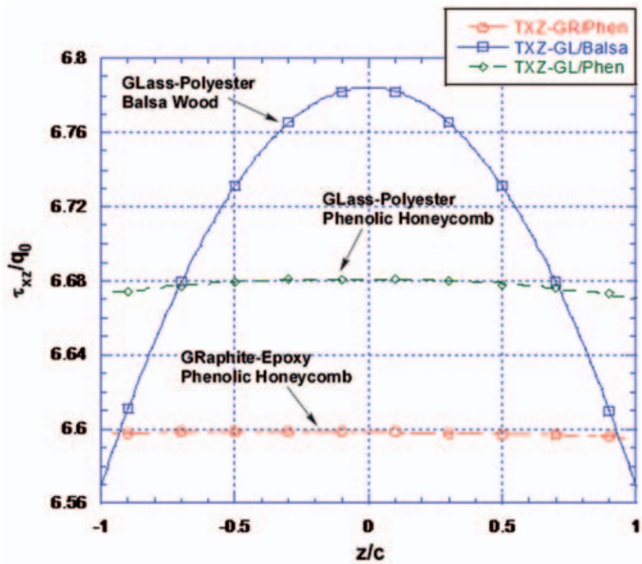

Figure 5. Through-thickness distribution in the core of the transverse shear stress, τ_{xz}, at $x = a/10$, for three face/core material combinations.

Conclusions

A three-dimensional elasticity solution for a sandwich beam/wide plate with negative discriminant orthotropic phases (resulting in complex conjugate roots) or positive discriminant but real negative roots is presented. This is a case frequently encountered in realistic sandwich construction. The solution is closed-form. This study completes Pagano's [3] original work, which was done for the positive discriminant with real positive roots orthotropic phases and for the isotropic phases. Results for a few representative face sheet and core material configurations are presented.

Acknowledgments

The financial support of the Office of Naval Research, Grant N00014-07-10373, and the interest and encouragement of the Grant Monitor, Dr. Y.D.S. Rajapakse, are both gratefully acknowledged.

Funding

This work was supported by the Office of Naval Research [grant number N00014-07-10373].

References

1. Lekhnitskii SG. *Theory of elasticity of an anisotropic elastic body*. San Francisco: Holden-Day, Inc., 1963.

2. Vlasov BF. *On one case of bending of rectangular thick plates*. Vestnik Moskovskogo Universiteta, 1957, Serieii'a Matematiki, mekhaniki, astronomii, fiziki, khimii, No. 2, p. 2534 (in Russian).
3. Pagano NJ. Exact solutions for composite laminates in cylindrical bending. *J Compos Mater* 1969; 3: 398–411.
4. Pagano NJ. Exact solutions for rectangular bidirectional composites and sandwich plates. *J Compos Mater* 1970; 4: 20–34.
5. Kardomateas GA. Elasticity solutions for a sandwich orthotropic cylindrical shell under external pressure, internal pressure and axial force. *AIAA J* 2001; 39: 713–719.

Appendix 1

Isotropic phases

In the event that one of the phases is isotropic (this is more common for the core) with extensional modulus E and Poisson's ratio ν, then the following relationships hold for the material constants:

$$c_{11} = c_{22} = c_{33} = E\frac{1-\nu}{(1-2\nu)(1+\nu)}, \tag{A1a}$$

$$c_{12} = c_{13} = c_{23} = c_{11}\frac{\nu}{1-\nu}\,; \quad c_{66} = c_{55} = c_{44} = c_{11}\frac{1-2\nu}{2(1-\nu)}\,. \tag{A1b}$$

In this case, we find that Δ vanishes and the solution to equation (10) consists of two equal roots, $\lambda_i = p^2$, $i = 1, 2$. Therefore, the solutions of (7) occurs in the form of two repeated pairs of roots, $s_i = \pm p$.

In this case, the displacement functions take the form:

$$U(z) = (a_{1u} + a_{3u}z)e^{pz} + (a_{2u} + a_{4u}z)e^{-pz}\,, \tag{A2a}$$

$$W(z) = (a_{1w} + a_{3w}z)e^{pz} + (a_{2w} + a_{4w}z)e^{-pz}\,. \tag{A2b}$$

where the a_{iu} and a_{iw}, $i = 1, 4$ are constants. Of the eight constants appearing in (A2), only four are independent. The various relations that exist among these constants are found by substituting (A2) and (5a) into the equilibrium relations (4), in which the relations (A1) for the isotropic material constants are used. In this way, we deduce the following four relations:

$$a_{3w} = a_{3u}; \quad a_{4w} = -a_{4u}, \tag{A3a}$$

$$a_{1w} = a_{1u} - \frac{3-4\nu}{p}(4\nu-3)a_{3u}, \tag{A3b}$$

$$a_{2w} = -a_{2u} - \frac{3-4\nu}{p}(4\nu-3)a_{4u}. \tag{A3c}$$

Hence, if we consider constants a_{1u}, a_{2u}, a_{3u}, and a_{4u} as independent, which for convenience we rename again as g_1, g_2, g_3, and g_4, respectively, the displacement u is in the form (14a) with the z-dependent coefficients defined as:

$$d_{u1} = e^{pz}\ ; \quad d_{u2} = e^{-pz}\ ; \quad d_{u3} = ze^{pz}\ ; \quad d_{u4} = ze^{-pz}. \tag{A4a}$$

and the displacement w is in the form (15a) where,

$$d_{w1} = e^{pz}\ ; \quad d_{w2} = -e^{-pz}, \tag{A4b}$$

$$d_{w3} = \left(z - \frac{3-4\nu}{p}\right)e^{pz}\ ; \quad d_{w4} = -\left(z + \frac{3-4\nu}{p}\right)e^{-pz}. \tag{A4c}$$

The corresponding stresses are derived by substituting the above displacement expressions into the strain–displacement and stress–strain relationships. The σ_{zz} is in the form (16a) with the z-dependent coefficients defined as:

$$b_{zz1} = \frac{E}{1+\nu}pe^{pz}\ ; \quad b_{zz2} = \frac{E}{1+\nu}pe^{-pz}, \tag{A5a}$$

and

$$b_{zz3} = \frac{E}{1+\nu}(-2 + 2\nu + pz)e^{pz}\ ; \quad b_{zz4} = \frac{E}{1+\nu}(2 - 2\nu + pz)e^{-pz}. \tag{A5b}$$

Next, τ_{xz} is in the form (17a) with the z-dependent coefficients defined as:

$$b_{xz1} = \frac{E}{1+\nu}pe^{pz}\ ; \quad b_{xz2} = -\frac{E}{1+\nu}pe^{-pz}, \tag{A6a}$$

$$b_{xz3} = \frac{E}{1+\nu}(-1 + 2\nu + pz)e^{pz}\ ; \quad b_{xz4} = \frac{E}{1+\nu}(-1 + 2\nu - pz)e^{-pz}\ , \tag{A6b}$$

Finally, σ_{xx} is in the form (18) with the z-dependent coefficients defined as:

$$b_{xx1} = -\frac{E}{1+\nu}pe^{pz}\ ; \quad b_{xx2} = -\frac{E}{1+\nu}pe^{-pz}, \tag{A7a}$$

$$b_{xx3} = -\frac{E}{1+\nu}(2\nu + pz)e^{pz}\ ; \quad b_{xx4} = \frac{E}{1+\nu}(2\nu - pz)e^{-pz}\ , \tag{A7b}$$

Appendix 2

Classical and first-order shear theories

Classical sandwich beam theory (without shear). The classical sandwich theory assumes that the core is transversely incompressible and the displacements of the top and bottom face sheets and care are the same. The governing differential equation is:

$$D_{11}\frac{\partial^4 w(x)}{\partial x^4} = \tilde{q}_0(x), \tag{A8}$$

where D_{11} is the bending stiffness per unit width of the beam.

In the general asymmetric case, the neutral axis of the sandwich section is defined at a distance e from the x-axis (Figure 1):

$$e\left(E_1^t f_t + E_1^b f_b\right) = E_1^t f_t\left(\frac{f_t}{2} + c\right) - E_1^b f_b\left(\frac{f_b}{2} + c\right). \tag{A9}$$

Therefore, the bending stiffness per unit width, D_{11}, is:

$$D_{11} = E_1^t\frac{f_t^3}{12} + E_1^t f_t\left(\frac{f_t}{2} + c - e\right)^2 + E_1^b\frac{f_b^3}{12} + E_1^t f_b\left(\frac{f_b}{2} + c + e\right)^2. \tag{A10}$$

For the load of (26a), the displacement is expressed as:

$$w(x) = W_0 \sin\frac{\pi x}{a} \ . \tag{A11}$$

Substituting into Equation (A8) leads to:

$$W_0 = \frac{q_0 a^4}{D_{11}\pi^4}. \tag{A12}$$

First-order shear sandwich beam theory. For the first-order shear model, if we let ψ be the shear deformation then the governing equations with shear effects can be written as:

$$D_{11}\psi_{,xx}(x) - \kappa D_{55}\left[\psi(x) + w_{,x}(x)\right] = 0 \ , \tag{A13}$$

$$\kappa D_{55}\left[\psi_{,x}(x) + w_{,xx}(x)\right] + \tilde{q}_0(x) = 0 \ , \tag{A14}$$

where $\kappa = 5/6$ is the shear correction factor and

$$D_{55} = G_{13}^c(2c) \ . \tag{A15a}$$

In some versions of the first-order shear model, the shear of the face sheets is included, i.e.

$$D_{55} = G_{13}^{c}(2c) + G_{13}^{t} f_t + G_{13}^{b} f_b. \tag{A15b}$$

Setting

$$w(x) = W_0 \sin\frac{\pi x}{a} \; ; \qquad \psi(x) = \Psi_0 \cos\frac{\pi x}{a}. \tag{A16}$$

with the load in the same manner as Equation (26a), and substituting in (A13) and (A14) leads to:

$$\Psi_0 = -\frac{L_{13}}{L_{11}L_{33} - L_{13}^2} q_0 \; ; \qquad W_0 = \frac{L_{11}}{L_{11}L_{33} - L_{13}^2} q_0 \; , \tag{A17}$$

where

$$L_{11} = D_{11}\frac{\pi^2}{a^2} + \kappa D_{55} \; ; \qquad L_{13} = \kappa D_{55}\frac{\pi}{a} \; ; \qquad L_{33} = \kappa D_{55}\frac{\pi^2}{a^2} \; . \tag{A18}$$